IEEE Access
Multidisciplinary | Rapid Review | Open Access Journal

Received May 21, 2018, accepted June 29, 2018, date of publication July 9, 2018, date of current version July 30, 2018.

Digital Object Identifier 10.1109/ACCESS.2018.2853637

Transient Stability Assessment Using Individual Machine Equal Area Criterion Part II: Stability Margin

SONGYAN WANG, JILAI YU, AND WEI ZHANG, (Member, IEEE)
School of Electrical Engineering and Automation, Harbin Institute of Technology, Harbin 150001, China
Corresponding author: Songyan Wang (wangsongyan@163.com)

ABSTRACT In the second part of this two-paper series, the stability margin of a critical machine and that of the system are first proposed, and then the concept of the nonglobal stability margin is illustrated. Based on the crucial statuses of the leading unstable critical machine and the most severely disturbed critical machine, the critical stability of the system from the perspective of an individual machine is analyzed. At the end of this paper, comparisons between the proposed method and classic global direct methods are demonstrated.

INDEX TERMS Transient stability, equal area criterion, individual machine energy function, partial energy function.

I. NOMENCLATURE

CCT	Critical clearing time
DLP	dynamic liberation point
DSP	dynamic stationary point
EAC	Equal area criterion
IMT	Individual-machine trajectory
LUM	the leading unstable machine
MDM	the most severely disturbed machine
MOD	Mode of disturbance
TSA	Transient security assessment
UEP	Unstable equilibrium point
3DKC	3-dimensional Kimbark curve
CDSP	DSP of the critical stable machine
CUEP	Controlling UEP
LOSP	Loss-of-synchronism point
IEEAC	Integrated extended EAC
IMEAC	Individual-machine EAC

II. INTRODUCTION

This is the second paper of a two-paper series dealing with power system transient stability by using the IMEAC. In the first paper [1], it is proved that EAC strictly holds for a critical machine, and the system operator may only focus on analyzing the stability of the critical machines. The mapping between IMEAC and the multimachine system trajectory is established because a critical machine becoming unstable in θ_i-f_i space is identical to the IMT becoming unstable in t-θ_i space. Further, the unity principle reveals that the system can be considered to be stable if all critical machines are stable, and the system can be considered to be unstable as long as any one critical machine is found to become unstable. These concepts intuitively demonstrate the mechanism of the proposed method in power system transient stability analysis.

References [2] and [3] can be seen as the two representative works in the history of individual-machine methods. In the two papers, Stanton pointed out that ''while some analysts think that this PEF application is obvious, others (notably Lyapunov global energy analysts) often object to the less than global point of view''. Stanton proposed some crucial conjectures and hypothesis about individual-machine methods. Especially, Stanton first stated that the multi-machine transient stability can be monitored in a ''machine-by-machine'' way. However, a limitation is that Stanton did not provide the definition of the stability margin of the system in the sense of an individual machine. In addition, although the concept of leading unstable machine was first given in the two papers, the mechanism of nonglobal monitoring was not fully explored. These unsolved issues caused confusion when using individual-machine methods in TSA and CCT computations, and they were not solved in later works of individual-machine methods [4], [5].

Following conclusions of the first paper, in this paper, first, the stability margin of a critical machine and that of the system are defined. The stability margin of the system is defined as a multidimensional vector that consists of

the stability margin of each critical machine in the system. Second, the important status of the most severely disturbed machine (MDM) and the leading unstable machine (LUM) are analyzed. According to the unity principle, the nonglobal stability margin is defined and its application in TSA is also demonstrated. It is proved that the stability judgment of the system can be independent of the calculation of the stability margin of the system. In addition, the proposed method allows system operators to neglect monitoring some critical machines when judging the stability of the system under certain circumstances. Third, the application of the proposed method in the computation of CCT is analyzed. We prove that the critical stability of the system is precisely identical to the critical stability of the MDM. At the end of the paper, the proposed method is compared with the CUEP method and the IEEAC method.

The contributions of this paper are summarized as follows:

(i) The stability margin of the system, which consists of the multiple stability margins of the critical machines of the system, is first defined in this paper, and this definition of a multidimensional vector enables the nonglobal transient stability monitoring in TSA;

(ii) The MDM and LUM are analyzed in this paper, and it is proven that they might be two different machines for some cases, which clarifies the historical misunderstanding in individual-machine methods that the MDM and LUM are the same machine;

(iii) According to the unity principle, it is proven that the critical stability state of only one or a few MDMs determines the critical stability of the system in this paper, and based on this, an approach to analyze the critical stability of the system using the MDM is proposed.

The remainder of the paper is organized as follows. In Section III, the definitions of the stability margin of a critical machine and that of the system are provided. In Section IV, the nonglobal stability margin is analyzed. In Section V, general procedures of the proposed method are provided. In Section VI, the application of the proposed method in TSA is demonstrated. In Section VII, the proposed method is utilized for CCT computation. In Section VIII and IX, the proposed method is compared with the CUEP method and the IEEAC method respectively. In Section X, further analysis of the not-all-critical-machine characteristic of the proposed method is provided. In Section XI, the jigsaw thinking in the proposed method is illustrated. Conclusions and discussions are provided in Section XII.

III. STABILITY MARGIN OF THE SYSTEM

A. STABILITY MARGIN OF A CRITICAL MACHINE

1) STABILITY MARGIN OF AN UNSTABLE CRITICAL MACHINE

Using the IMEAC, the stability margin of an unstable critical machine can be intuitively defined as follows:

$$\eta_i = (A_{DECi} - A_{ACCi})/A_{ACCi} \tag{1}$$

where $A_{ACCi} = -\int_{\theta_i^0}^{\theta_i^c} \left[-f_i^{(F)}\right] d_{\theta_i}, A_{DECi} = \int_{\theta_i^c}^{\theta_i^{DLP}} \left[-f_i^{(PF)}\right] d_{\theta_i}$

A_{ACCi} and A_{DECi} are acceleration area and deceleration area of the machine, respectively. The margin definition in Eq. (1) ensures that $\eta_i < 0$ if a critical machine becomes unstable, as A_{DECi} is smaller than A_{ACCi} for an unstable critical machine [1].

2) STABILITY MARGIN OF A STABLE CRITICAL MACHINE

For a stable critical machine, the A_{DECi} equals to the A_{ACCi} in the actual Kimbark curve of the machine [1]. However, the deceleration area of the machine may still possess a certain ''margin'' after the DSP occurs even though the acceleration energy during the fault-on period is already totally absorbed at the DSP, as shown in Fig. 1.

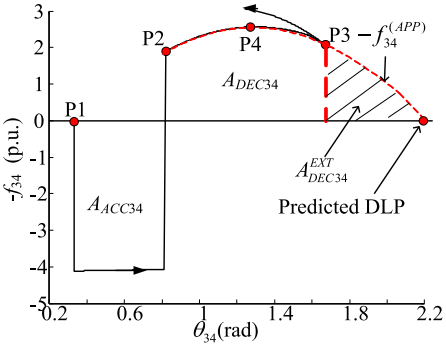

FIGURE 1. Stability margin of a stable critical machine (Machine 34, [[TS-1, bus-34, 0.180s]).

For a stable critical machine, the Kimbark curve of the critical machine prior to the DSP can be approximated by a quadratic function:

$$-f_i^{(APP)} = a_i\theta_i^2 + b_i\theta_i + c_i \tag{2}$$

The parameters in Eq. (2) can be identified via three points, i.e., the fault clearing point (P2), the DSP (P3) and the point with maximum -f_i (P4). Further, the stability margin of a stable critical machine can be defined as follows:

$$\eta_i = (A_{DECi} + A_{DECi}^{EXT} - A_{ACCi})/A_{ACCi} = A_{DECi}^{EXT}/A_{ACCi} \tag{3}$$

where

$$A_{DECi}^{EXT} = \int_{\theta_i^{DSP}}^{\theta_i^{DLP(PRED)}} [-f_i^{(APP)}] d_{\theta_i}, \quad A_{DECi} = A_{ACCi}$$

A_{DECi}^{EXT} extended deceleration area

$\theta_i^{DLP(PRED)}$ predicted DLP

In Eq. (3), the margin definition ensures that $\eta_i > 0$ if a critical machine is stable and $\eta_i = 0$ if a critical machine is critical stable.

Considering that the application of $-f_i^{(APP)}$ may result in an approximation error, in the following analysis, the Kimbark curve of a stable critical machine prior to the DSP still uses the original Kimbark curve, and $-f_i^{(APP)}$ is only used for the computation of A_{DECi}^{EXT}.

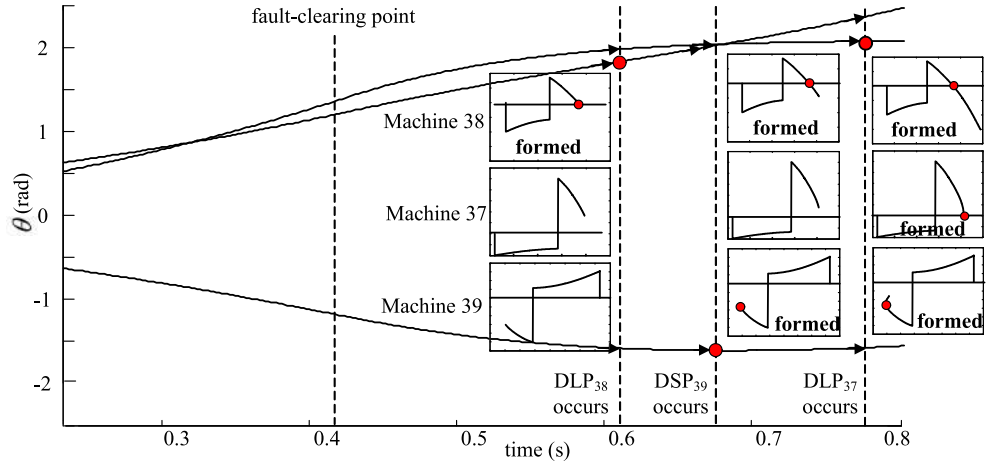

FIGURE 2. Machine-by-machine stability judgment along the post-fault system trajectory [TS-1, bus-2, 0.43 s].

B. DEFINITION OF THE STABILITY MARGIN OF THE SYSTEM

Since the system operators focus on the swing stability of each critical machine in parallel in TSA, they may only target the IMEAC of each critical machine. Therefore, the stability margin of the system can be defined as a multidimensional vector comprised of the margins of all the critical machines in the system:

$$\boldsymbol{\eta}_{\text{sys}} = [\eta_i] \quad i \in \Omega_{\text{c}} \tag{4}$$

where Ω_{c} is the set of all critical machines in the system.

Following the unity principle, the stability judgment of the system can be given as follows: all $\eta_i > 0$ means that the system is stable; one or a few $\eta_i = 0$ with the rest of $\eta_i > 0$ means that the system is critical stable; and one or more $\eta_i < 0$ means that the system becomes unstable.

C. MACHINE-BY-MACHINE MARGIN CALCULATION

From the analysis in the first paper, along the post-fault system trajectory, the DLPs and DSPs of the critical machines occur machine-by-machine. Since the actual shape of the Kimbark curve of a machine in a complete individual-machine swing could be formed only when the DSP or DLP occurs, accordingly, the η_i of each critical machine should also be calculated in a ''machine-by-machine'' way. A demonstration of calculating the stability margin of the system during TSA is shown in Fig. 2.

As shown in Fig. 2, after fault clearing the system operator only monitors Machines 37, 38 and 39, as they are critical machines. Along the post-fault system trajectory, the system operator may focus on the following instants.

DLP_{38} occurs (0.614 s): Machine 38 is judged as unstable, and η_{38} is obtained. However, $\boldsymbol{\eta}_{\text{sys}}$ is unknown due to the lack of η_{37} and η_{39}.

DSP_{39} occurs (0.686 s): Machine 39 is judged as stable, and η_{39} is obtained. $\boldsymbol{\eta}_{\text{sys}}$ is unknown due to the lack of η_{37}.

DLP_{37} occurs (0.776 s): Machine 37 is judged as unstable, and η_{37} is obtained. $\boldsymbol{\eta}_{\text{sys}}$ is obtained.

The computation of the margin of each critical machine is shown in Table 1.

TABLE 1. Stability margin of critical machines.

Machine No.	A_{ACCi} (p.u.)	A_{DECi} (p.u.)	A_{DECi}^{EXT} (p.u.)	η_i
38	1.33	0.54	N/A	-0.594
39	3.22	3.22	1.57	0.489
37	2.09	2.08	N/A	-0.005

Based on the margins of all critical machines in the system shown in Table 1, $\boldsymbol{\eta}_{\text{sys}}$ is finally computed as [-0.594, 0.489, -0.005].

As for the online security control, the controlling objective is to ensure that the entire system maintains stable, i.e., all critical machines in the system should be maintained stable (the controlling action should be deployed immediately once an unstable critical machine is observed). Thereby, the security control based on the IMEAC method strongly relies on the computation of $\boldsymbol{\eta}_{\text{sys}}$. However, under certain circumstances it is possible that the system operator is *only* interested in the stability state of only one or a few of the most severely disturbed critical machines rather than all critical machines. This also indicates that transient stability of the power system can be analyzed ''nonglobally''.

IV. NONGLOBAL STABILITY MARGIN

A. STATUS OF A CRITICAL MACHINE

During the post-fault transient period, two specific critical machines are crucial, which can partially represent the transient stability characteristics of all critical machines in the system. The first one is the most severely disturbed machine (MDM), and the second one is the leading unstable machine (LUM).

1) MDM

The MDM is defined as the critical machine with the lowest stability margin.

$$\eta_{MDM} = \min[\boldsymbol{\eta}_{\text{sys}}] \tag{5}$$

Notice that the MDM can be confirmed *only when* the margin of the last critical machine is obtained during the time horizon, because the margin of the system should be obtained in a machine-by machine way, as analyzed in Section III.

2) LUM

The LUM is defined as the unstable critical machine whose DLP occurs first among all unstable critical machines

$$t_{DLP_{LUM}} = \min[t_{DLP_i} | i \in \Omega_c] \tag{6}$$

The reasons why the MDM and LUM are important for transient stability analysis are as follows.

a: THE STABILITY STATE OF THE MDM IS IDENTICAL TO THE STABILITY STATE OF THE SYSTEM

Following the unity principle, the system can be judged as stable if the MDM is stable, the system can be judged as critical stable if the MDM is critical stable, and the system can be judged as unstable if the MDM becomes unstable. Thus, the stability state of the MDM is identical to the stability state of the system.

b: THE LEADING LOSP IS IDENTICAL TO THE DLP OF THE LUM

The LUM is the first-going-unstable critical machine that separates from the system. Once the LUM appears, the system operator can ascertain that the system has become unstable, and the DLP of the LUM can therefore be defined as the leading LOSP.

From the analysis above, the two crucial transient stability characteristics of a multimachine system, i.e., the stability state of the system and the leading LOSP, respectively, are fully embodied in the MDM and LUM.

For most unstable cases, the MDM and LUM may be the same machine. However, for some cases, it is still possible that the MDM and LUM might be two different machines.

B. DEFINITION OF NONGLOBAL STABILITY MARGIN

1) NONGLOBAL STABILITY MARGIN FOR TSA (THE SYSTEM OPERATOR MISSES MONITORING SOME CRITICAL MACHINES)

If the critical machines in the system are not all monitored, the stability margin of the system could only be depicted in an incomplete nonglobal form, as follows:

$$\boldsymbol{\eta}_{\text{non}} = [\eta_i] \quad i \in \Omega_{\text{non}} \quad \Omega_{\text{non}} \subset \Omega_c \tag{7}$$

where Ω_{non} is the set of nonglobally monitored critical machines.

In Eq. (7), $\boldsymbol{\eta}_{\text{non}}$ is defined such that only parts of the critical machines are monitored. Under this not-all-critical-machine monitoring circumstance, $\boldsymbol{\eta}_{\text{sys}}$ cannot be evaluated since it is defined by all critical machines. However, following the unity principle, it is still possible that the stability state of the system can be judged as long as any one unstable critical machine is included in $\boldsymbol{\eta}_{\text{non}}$.

The analysis above is crucial because it reveals that, for the proposed method, the unity principle allows the following

"*The stability judgment of the system is independent of the acquisition of the stability margin of the system.*"

A demonstration of the nonglobal monitoring is shown in Fig. 3. Machine 38 is not monitored by the system operator.

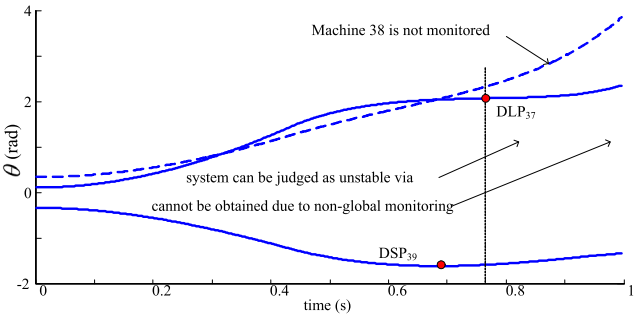

FIGURE 3. Demonstration of nonglobal monitoring [TS-1, bus-2, 0.43 s].

In this case, $\boldsymbol{\eta}_{\text{sys}}$ cannot be obtained. However, the system can still be judged as unstable once DLP_{37} occurs.

In fact, judging the stability of the system by using only one unstable critical machine and *neglecting* the rest of the critical machines is a type of "missing transient information". However, once the MDM and LUM are monitored and both machines are included in Ω_{non}, the system operator is still able to grasp the key transient information of the system, i.e., the stability state and leading LOSP of the system. Tolerating the missing transient information can be seen as a distinctive characteristic of the proposed method, making it quite robust in the TSA.

2) NONGLOBAL STABILITY MARGIN FOR CCT COMPUTATION (THE SYSTEM OPERATOR INTENTIONALLY FOCUSES ON THE MDM)

Following the definition of the MDM, the stability state of the MDM is identical to the stability state of the system. From the perspective of individual-machine analysts, the main role of the MDM is its application in CCT computation because

"*the critical stability of the system is fully determined by the critical stability of the MDM, according to the unity principle.*"

Numerous simulations have proven that the MDM will not change around the critical stability state. Therefore, during iterations of the fault-clearing time when computing the CCT, the system operator may target the MDM in the first iterations. Then, the system operator may only monitor the MDM without observing the other critical machines. Under this circumstance, the nonglobal stability margin for the CCT computation can be directly depicted as follows:

$$\boldsymbol{\eta}_{\text{non}} = \eta_{\text{MDM}} \tag{8}$$

In Eq. (8), the stability of the whole system is fully represented by that of the MDM when computing the CCT of the system. Detailed analysis about the CCT computation is provided in Section VII.

V. PROCEDURES OF THE PROPOSED METHOD IN THE TRANSIENT STABILITY ANALYSIS

A. APPLICATION OF THE PROPOSED METHOD IN THE TSA

For a certain occurred fault in the TSA, the procedures of parallel monitoring using the proposed method are outlined as follows.

Step 1: Monitor all critical machines in parallel after fault clearing.

Step 2: Along the post-fault system trajectory, the stability of all critical machines in the system is judged in a machine-by-machine way. The stability of the machine is identified via the occurrence of the DLP or DSP, and η_i of the critical machine is calculated via the IMEAC.

Step 3: If one or more DLPs occur, the first DLP that occurs is defined as the leading LOSP, and the system is immediately judged as unstable. Meanwhile, the machine with the first occurring DLP is defined as the LUM.

Step 4: If no DLP occurs and, instead, DSPs occur one after another until the Kimbark curve of the last critical machine is formed, the system can be judged as stable when the last DSP occurs.

Step 5: At the instant that the Kimbark curve of the last critical machine is formed, the MDM is identified and $\boldsymbol{\eta}_{\text{sys}}$ is finally obtained.

The procedures of nonglobal monitoring are almost the same as those of parallel monitoring. The only difference is that the critical machines are not all monitored.

B. APPLICATION OF THE PROPOSED METHOD IN THE CCT COMPUTATION

The procedures of the CCT computation using the proposed method are outlined as follows.

Step 1: For the first few iterations with the system being stable, the MDM is identified by finding the minimum η_i among all stable critical machines in the system.

Step 2: Once the MDM is identified, only the MDM is monitored in the following iterations.

Step 3: If $\eta_{\text{MDM}} > 0$ when the fault clearing time is t_u and $\eta_{\text{MDM}} < 0$ when the fault clearing time is $t_u + \Delta t$, then t_u is set as the CCT of the system.

VI. SIMULATIONS OF THE PROPOSED METHOD IN TSA

A. PARALLEL MONITORING

Here, the small-scale test network TS-1 is provided first to systematically demonstrate the application of the proposed method in TSA. The fault is [TS-1, bus-21, 0.370 s]. The system trajectory is shown in Fig. 4.

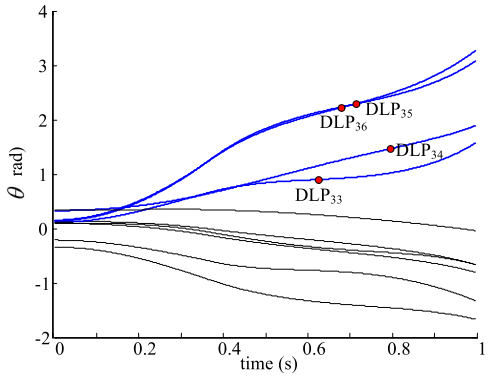

FIGURE 4. System trajectory [TS-1, bus-21, 0.37 s].

After fault clearing, Machines 33-36 are defined as critical machines. Using the proposed method, along time horizon, the system operators focus on the following instants.

DLP_{33} occurs (0.611 s): (i) Machine 33 is judged as unstable, and η_{33} is obtained. (ii) Machine 33 is identified as the LUM. (iii) DLP_{33} is identified as the leading LOSP, and the system is judged as unstable.

DLP_{36}—DLP_{35} occur (0.671 s, 0.710 s): The corresponding critical machines are judged as unstable, and their η_i values are obtained one after another.

DLP_{34} occurs (0.795 s): (i) Machine 34 is judged as unstable, and η_{34} is obtained. (ii) Machine 34 is identified as the MDM. (iii) $\boldsymbol{\eta}_{\text{sys}}$ is obtained.

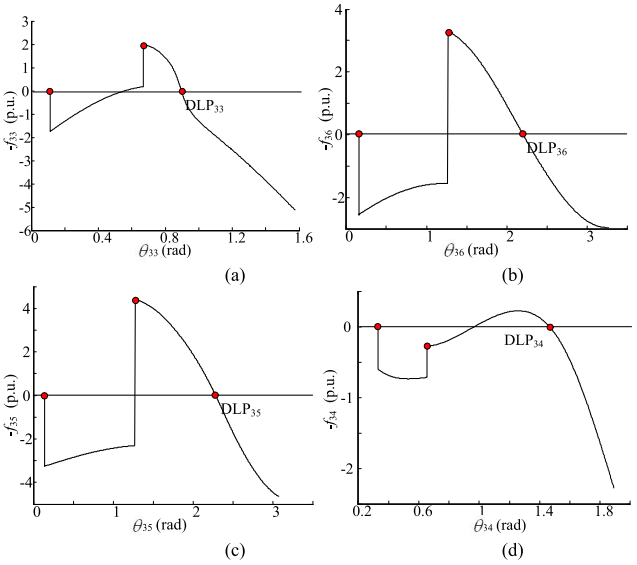

FIGURE 5. Simulated Kimbark curves [TS-1, bus-21, 0.370s]. (a-d) Kimbark curves of Machines 33, 36, 35 and 34.

The Kimbark curves of the critical machines are shown in Figs. 5 (a)–(d). The stability margins of the critical machines are shown in Table 2.

TABLE 2. Stability margins of critical machines

Machine No.	A_{ACCi} (p.u.)	A_{DECi} (p.u.)	η_i
33	0.34	0.33	-0.03
36	2.09	1.83	-0.12
35	3.03	2.82	-0.07
34	0.2816	0.0717	-0.75

As shown in Table 2, at the moment the DLP_{34} occurs, η_{sys} is finally calculated as [-0.03, -0.12, -0.07, -0.75].

B. MDM AND LUM

For the case shown in Fig. 4, Machines 34 and 33 are identified as the MDM and LUM, respectively. The occurrences of the MDM and LUM along the time horizon are shown in Fig. 6.

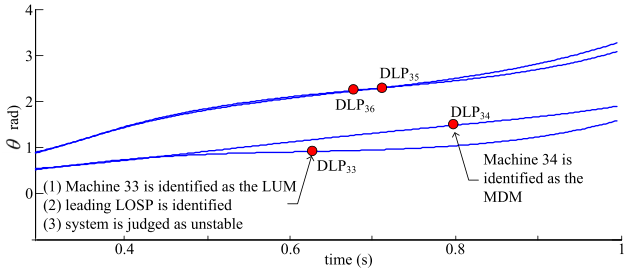

FIGURE 6. Identification of the MDM and LUM [TS-1, bus-21, 0.37s].

The result shown in Fig. 6 validates that the MDM and LUM might not be the same machine under certain circumstances. Especially, for the case in Fig. 6, Machine 33 possesses the highest margin but is the first one to go unstable, whereas Machine 34 possesses the lowest margin but is the last one to become unstable. Machine 34 is still decelerating at the instant of DLP_{33} (0.611 s), which indicates that there might be little correlation between the MDM and LUM in some simulation cases.

From the simulation results above, one can see that along the actual post-fault system trajectory, the MDM can be identified only when the stability margin of the last critical machine is calculated because the determination of the minimum margin should be based on the acquisition of the stability margin of all the critical machines. Comparatively, the identification of the LUM may be more ''important'' than the MDM in TSA because both the instability of the system and the leading LOSP can be immediately identified when the LUM occurs without waiting for the occurrence of the MDM (still notice that the MDM can be confirmed only when the margin of the last critical machine is calculated along the time horizon). In addition, the system operators should already be prepared to take proactive controlling actions at the instant when the leading LOSP occurs.

C. NOT-ALL-CRITICAL-MACHINES MONITORING

For the case in Fig. 4, assume that the system operator neglects monitoring Machine 34 after the fault clearing; then, only three critical machines are monitored.

Under this circumstance, the instability of the system can still be correctly identified when DLP_{33} occurs. Later, Machines 36 and 35 are both judged as unstable consecutively. Meanwhile, at the instant of DLP_{35}, the η_{non} is finally calculated as [-0.03, -0.12, -0.07, N/A].

From the analysis above, although η_{sys} cannot be obtained due to the unmonitored Machine 34, both the stability state and the leading LOSP of the system can still be correctly identified via the three monitored machines, which indicates that η_{non} could ''partially'' represent the margin of the system.

VII. APPLICATION OF THE PROPOSED METHOD IN CCT COMPUTATION

In this section, a simulation case is provided to illustrate the relationship between the critical stability of the critical machines and that of the system. The CCT of the system for the fault [TS-1, bus-19] is 0.215 s according to the time-domain simulation. Machines 33, 34 and 39 are critical machines. The critical stable and critical unstable system trajectories are shown in Figs. 7(a) and (b), respectively. The Kimbark curves of critical machine 34 in both cases are shown in Figs. 8(a) and (b), respectively.

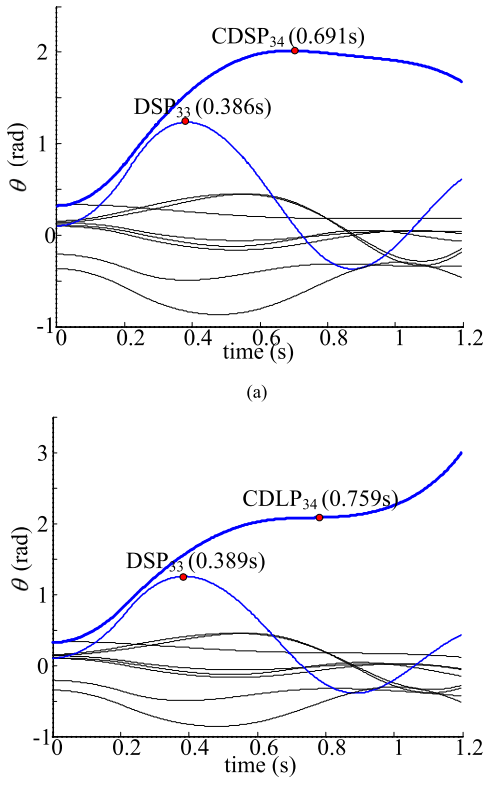

FIGURE 7. Simulated system trajectory. (a) Critical stable case. (b) Critical unstable case.

In Figs. 7(a) and (b), we observe the critical stable and critical unstable system trajectories from the perspective of the individual machine. When the fault clearing time is 0.215 s, Machine 34 (i.e., IMT_{34}) is critical stable, whereas Machines 33 and 39 are marginal stable; thus, the system trajectory is kept stable, as shown in Fig. 8(a). When the fault clearing time is slightly increased to 0.216 s, Machines 33 and 39 are still marginally stable. However, Machine 34 starts separating from the system at $CDLP_{34}$ and finally becomes unstable, causing the system to become unstable, as shown in Fig. 8(b). From the analysis above, the critical stability of Machine 34 fully determines the critical stability of the system, and the

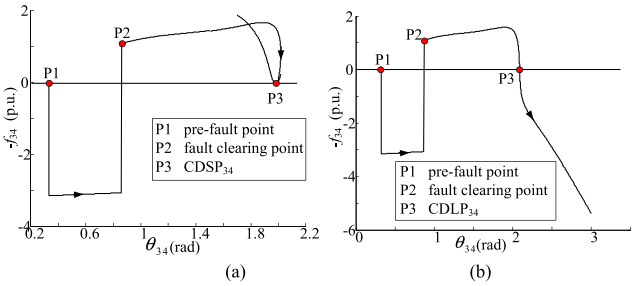

FIGURE 8. Kimbark diagram of Machine 34. (a) Critical stable case. (b) Critical unstable case.

real inflection point of the critically stable system trajectory is $CDSP_{34}$. This validates the analysis in Section IV B.

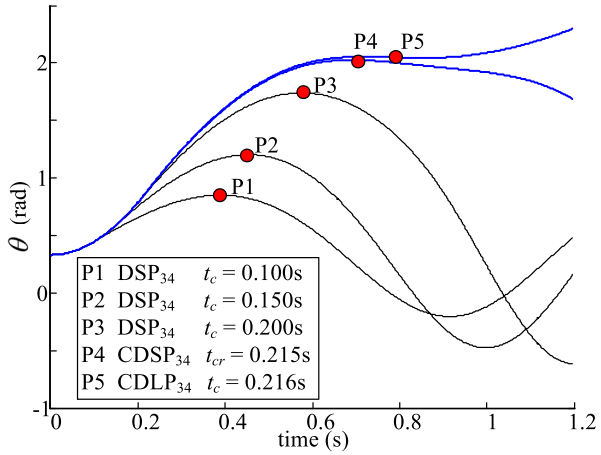

FIGURE 9. The variance of the IMT_{34} with the change of the fault clearing time.

The variation in the IMT_{34} with the change in fault clearing time is shown in Fig. 9. The variance of the stability margins of the critical machines with different CTs are shown in Table 3 (notice that $-f_i$ of the critical stable machine might not be zero due to simulation errors).

TABLE 3. Variations in the stability margins of critical machines with fault clearing time.

CT (s)	Machine No.	η_i	MDM No.
	34	0.112	
0.213	33	1.055	34
	39	1.440	
	34	0.104	
0.214	33	1.047	34
	39	1.428	
	34	0.068	
0.215	33	1.038	34
	39	1.416	
	34	-0.001	
0.216	33	1.026	34
	39	1.405	
	34	-0.005	
0.217	33	1.021	34
	39	1.392	

As shown in Table 3, after the first few iterations, it can be confirmed that Machine 34 is the MDM, as η_{34} is much lower than η_{33} and η_{39}; thus, the system operator may only monitor Machine 34 in the followed iterations, as analyzed in Section IV (η_{33} and η_{39} are also shown in the table to demonstrate the variation of the margin). Later, with the increase in the fault clearing time, Machine 34 is still maintained as the MDM. When the fault clearing time is 0.216 s, η_{34} changes from positive to negative, and Machine 34 becomes critically unstable, which causes the system to become critically unstable. This validates that it is only the critical stability of Machine 34 that determines the critical stability of the system.

For some cases, it is possible that some critical machines might be highly correlated, and they may all change from being critically stable to being critically unstable, as shown in Fig. 10.

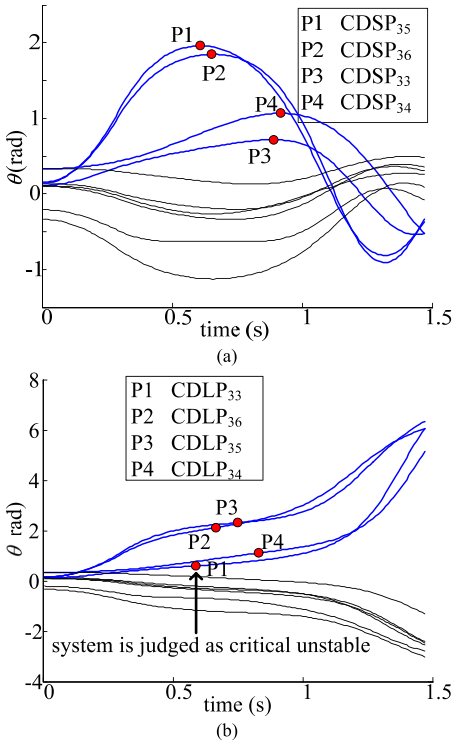

FIGURE 10. Simulated system trajectory [TS-1, bus-22, 0.295s], [TS-1, bus-22, 0.296s]. (a) Critical stable case. (b) Critical unstable case.

For the case in Fig. 10, Machines 33-36 are all critically stable at 0.295 s, and they should all be determined as MDMs and thus should be monitored in parallel. However, the critical instability of the system can be identified once the leading LOSP occurs without waiting for the occurrence of other DLPs. For instance, in this case, Machines 33-36 all become critically unstable when the fault clearing time is 0.296 s, yet the critical instability of the system can be immediately identified when the leading LOSP ($CDLP_{33}$) occurs at 0.580 s, as shown in Fig. 10(b).

Detailed calculations of the CCT in different test systems are shown in Table 4. The simulation step-size is set as 0.01 s. The results reveal that the computed CCT is precisely identical to the time domain simulations.

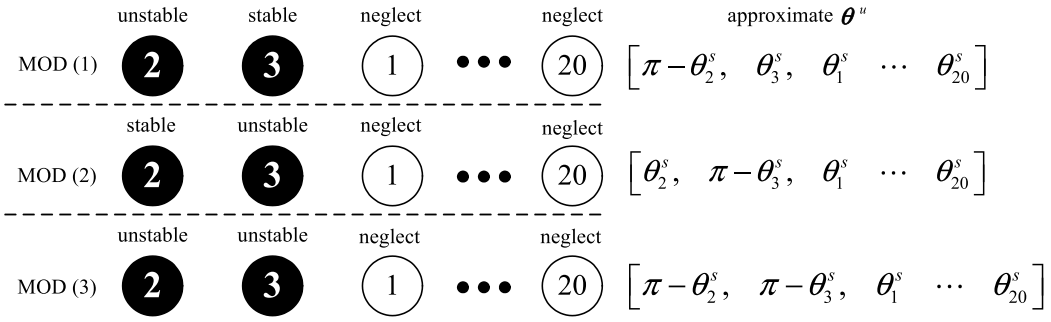

FIGURE 11. Possible MODs in the CUEP method.

TABLE 4. Calculations of CCT using the proposed method.

Fault location	Simulation (s)	Proposed method (s)	MDM No.	LUM No.
*TS-1, bus-34	0.20	0.20	34	34
*TS-1, bus-35	0.30	0.30	35, 36	36
*TS-1, bus-36	0.26	0.26	36	36
*TS-1, bus-37	0.24	0.24	37	37
TS-1, bus-4	0.44	0.44	31, 32	32
TS-1, bus-15	0.49	0.49	33-36	33
TS-1, bus-21	0.35	0.35	33-36	33
TS-1, bus-24	0.37	0.37	33-36	33
*TS-2, bus-10	0.19	0.19	2	2
*TS-2, bus-12	0.50	0.50	2	2
*TS-2, bus-25	0.34	0.34	4, 5	5
*TS-2, bus-40	0.57	0.57	8	8
*TS-2, bus-66	0.34	0.34	14	14
TS-2, bus-5	0.27	0.27	2	2
TS-2, bus-64	0.71	0.71	12	12
TS-2, bus-104	0.37	0.37	20	20

('*' Fault occurs at the terminal of the machine; "MDM No." the MDM when the system is critically stable; "LUM No" the LUM when the system becomes critically unstable)

VIII. COMPARISON BETWEEN THE CUEP METHOD AND THE PROPOSED METHOD

A. CUEP METHOD

The analysis in this section is fully based on the classic simulation cases in [6]. All parameters of the CUEP method follow the forms in [6]. The critical unstable case is set as [TS-2, bus-12, 0.510 s] [6]. Machines 2 and 3 are critical machines, with only Machine 2 becoming critically unstable in this case.

In the CUEP method, Fouad assumed that only critical machines might become unstable, and the concept of "approximate $\boldsymbol{\theta}^u$" is proposed to initiate the CUEP. To be specific, for the case above, Fouad assumed that only Machines 2 and 3 might become unstable. In this way, there are only three types of possible combinations of the MODs, as shown in Fig. 11.

As shown in Fig. 11, the approximate $\boldsymbol{\theta}^u$s for initiation are $\underline{\boldsymbol{\theta}}_2^u$, $\underline{\boldsymbol{\theta}}_3^u$ and $\underline{\boldsymbol{\theta}}_{2,3}^u$ [6]. Further, the CUEP and the corresponding real MOD are identified via the computation of the lowest global critical energy. In this case, the CUEP is computed as $\theta_{2,\mathrm{CUEP}} = 2.183$ rad and the real MOD is finally identified as only Machine 2 becoming unstable [6].

B. PROPOSED METHOD

Compared with the CUEP method that generates possible MODs first and then identifies the real MOD via the calculation of CUEP, the proposed method works in a more intuitive way because the proposed method directly monitors the IMTs of Machines 2 and 3 in parallel, as shown in Fig. 12. The simulation results show that DSP_3 and DLP_2 occur at 0.613 s and 0.948 s, respectively. The Kimbark curves of Machines 2 and 3 are shown in Figs. 13(a) and (b), respectively. The stability margins of Machines 2 and 3 are shown in Table 5.

From the analysis above, Machine 3 is judged as stable at DSP_3. Later, Machine 2 is judged as unstable at DLP_2, which directly causes the system to become unstable. Thus, the MOD is identified via the stability judgment of each critical machine without computing the CUEP.

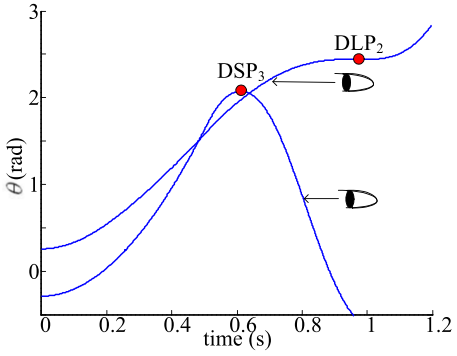

FIGURE 12. IMTs of Machines 2 and 3.

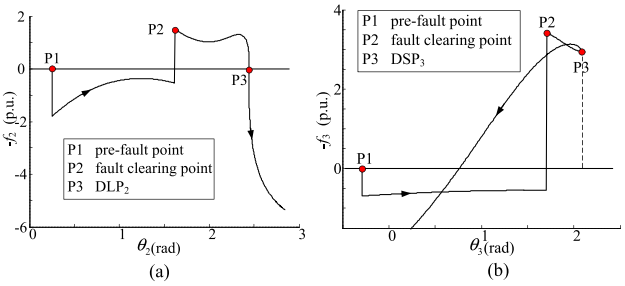

FIGURE 13. Simulated Kimbark curves. (a) Machine 2. (b) Machine 3.

TABLE 5. Stability margins of the critical machines.

No.	A_{ACCi} (p.u.)	A_{DECi} (p.u.)	A_{DECi}^{EXT} (p.u.)	η_i
Machine 2	0.97	0.96	N/A	-0.01
Machine 3	1.17	1.17	1.03	0.88

In fact, the computation of the stability margin of the system in the proposed method is identical to the classical concept of MOD as the stability state of all critical machines (no matter they are stable or not) should be obtained. Yet, since *the stability judgment of the system is independent of the acquisition of the stability margin of the system* as analyzed in Section IV B, it is obvious that the stability judgment of the system can be independent of MOD. For instance, in this case the system can be judged as unstable once Machine 2 is judged as unstable without monitoring Machine 3. Under this circumstance, although the MOD is unknown, the stability of the system is already identified.

IX. COMPARISON BETWEEN IEEAC METHOD AND PROPOSED METHOD

A. TEST BED

In this section, comparisons between the IEEAC method and the proposed method are provided to demonstrate the application of the proposed method when identifying the inter-area instability in TSA. The TS-3 is a practical 2766-bus, 146-unit interconnected system, with 8 wind power plants being integrated at the east of the grid. SYSTEM_LC is a regional system with 8 units, while SYSTM_SD is a main system with 138 units. SYSTEM_LC and SYSTM_SD are connected through a 500-kV double-AC transmission line. A five-order dynamic generator model with excitation and governor is utilized for the simulation. The load consists of the constant power load, constant impedance load, composite load and electric motor. The geographical layout of the interconnected system is shown in Fig. 14. The fault location is set at 90% of Line LIAOC_TANZ, which is close to TANZ. A three-phase short circuit event occurs at 0.00 s and is cleared at 0.22 s (CCT is 0.16 s). In this case, all machines in SYSTEM_LC accelerate with respect to SYSTEM_SD after the fault is cleared; thus, the separation mode of the interconnected system is a typical inter-area instability mode.

B. IEEAC METHOD

The simulated rotor angles of the interconnected system in synchronous reference are shown in Fig. 15.

For simplification, Ω_{n_LC} is defined as the set with [Gen. #XW, Gen. #HY, Gen. #CP, Gen. # XYRD], Ω_{s_LC} is defined as the set with [Gen. #LC1, Gen. #LC2, Gen. #LCR1, Gen. #LCR2], and Ω_{SD} is defined as the set with all machines in SYSTEM_SD. Using the IEEAC method, all machines in the interconnected system after fault clearing are separated into the critical group Ω_A and the noncritical group Ω_S. The possible group separation modes are given as follows:

Mode 1: Ω_A is set as Ω_{n_LC}, and Ω_S is set as $\Omega_{s\_LC} \cup \Omega_{SD}$;

Mode 2: Ω_A is set as $\Omega_{n\_LC} \cup \Omega_{s\_LC}$, and Ω_S is set as Ω_{SD}.

After calculating the stability margin of the OMIB system for the above two modes, Mode 2, whose OMIB system possesses a lower margin, is finally identified as the dominated group separation mode. In this mode, eight machines

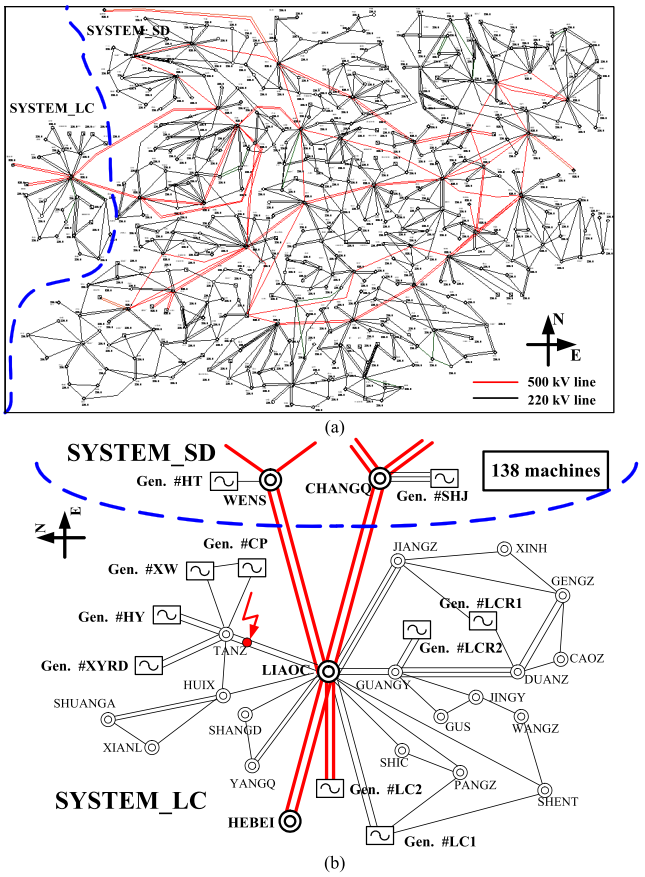

FIGURE 14. Geographical layout of the interconnected system. (a) Full view of the interconnected system. (b) Geographical layout of SYSTEM_LC.

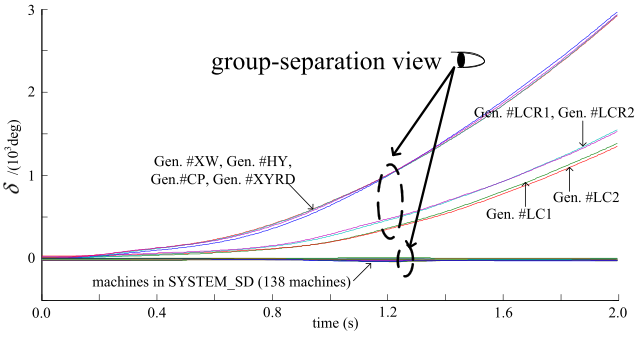

FIGURE 15. Rotor angles of the interconnected system in synchronous reference [TS-3, line-LIAOC_TANZ, 0.22s].

in $\Omega_{n\_LC} \cup \Omega_{s\_LC}$, and 138 machines in Ω_{SD} are equated as Machine A and Machine S, respectively. The Kimbark curve of the equated OMIB system is shown in Fig. 16. Notice that the equivalent P_m in the figure is not a horizontal line as the governors are deployed.

From Fig. 16, the Kimbark curve of the OMIB system goes across dynamic saddle point, i.e., the LOSP defined in IEEAC method at 0.89 s. At the moment when the dynamic saddle point occurs, the interconnected system is judged to become unstable, the inter-area instability is identified, and

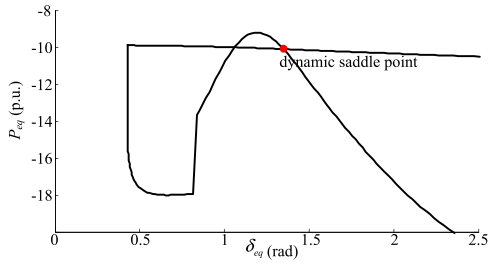

FIGURE 16. Kimbark curve of the OMIB system.

the stability margin of the interconnected system η_{OMIB} is also obtained.

C. PROPOSED METHOD (PARALLEL MONITORING)

Using the proposed method, the rotor angles of the interconnected system are first depicted in the COI reference, as shown in Fig. 17.

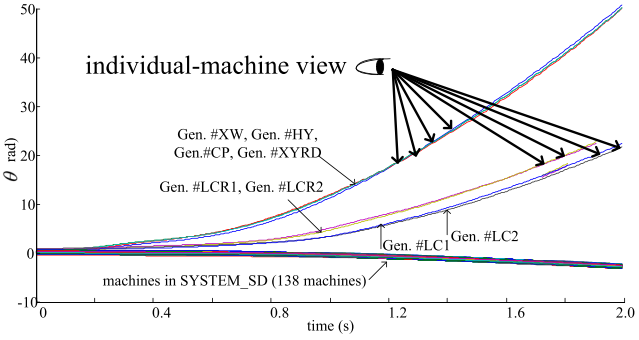

FIGURE 17. Rotor angles of the interconnected system in the COI reference [TS-3, line-LIAOC_TANZ, 0.22 s].

After fault clearing, all machines in SYSTEM_LC are identified as critical machines. Unlike the IEEAC method that separates all machines in the interconnected system into two groups, using the proposed method, the system operator monitors all critical machines in SYSTEM_LC in parallel, as shown in Fig. 17. The occurrence of the DLPs of these critical machines along the time horizon is shown in Fig. 18. The Kimbark curves of Gen. #XYRD and Gen. #LCR2 are shown in Figs. 19(a) and (b), respectively.

According to Fig. 18, along the time horizon, the system operator focuses on following instants.

DLP_{XYRD} occurs (0.79 s): Gen. #XYRD is judged as unstable.

DLP_{HY}—DLP_{LC2} occur (from 0.80 s to 1.03 s): The corresponding critical machines are judged as unstable consecutively.

DLP_{LC1} occurs (1.07 s): Gen. #LC1 is judged as unstable.

The stability of the system is judged as follows:

DLP_{XYRD} occurs (0.79 s): $\mathrm{DLP_{XYRD}}$ is identified as the leading LOSP, and the interconnected system is judged as unstable. However, the inter-area instability cannot be identified because the instability of the other critical machines in SYSTEM_LC is still unknown.

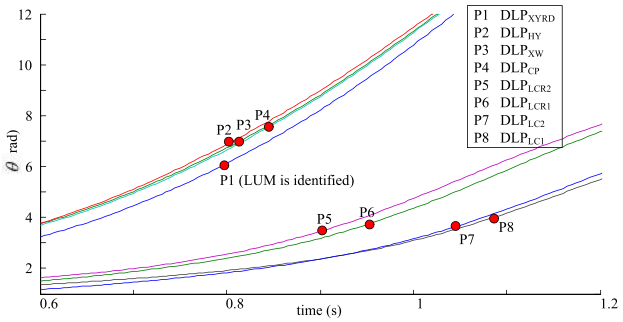

FIGURE 18. Occurrence of DLPs along the time horizon.

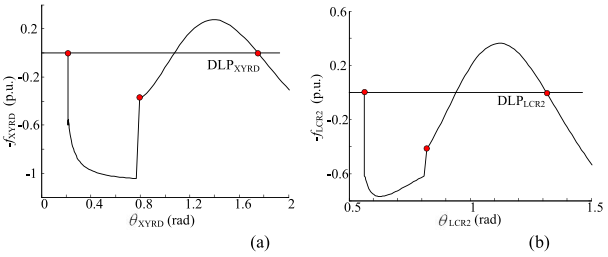

FIGURE 19. Simulated Kimbark curves. (a) Gen. #XYRD. (b) Gen. #LCR2.

DLP_{LC1} occurs (1.07 s): The inter-area instability is identified because all critical machines in SYSTEM_LC are judged as unstable at the instant, and $\boldsymbol{\eta}_{\mathrm{sys}}$ is finally obtained.

From the analysis above, using the proposed method, the *instability* of the interconnected system can be judged earlier than with the IEEAC method ($\mathrm{DLP_{XYRD}}$ occurs earlier than dynamic saddle point), yet the *inter-area instability* is identified later than with the IEEAC method ($\mathrm{DLP_{LC1}}$ occurs later than dynamic saddle point). In addition, in the IEEAC method, the stability judgment of the system, identification of the inter-area instability and η_{OMIB} are obtained simultaneously when the dynamic saddle point occurs, as demonstrated in Fig. 16. Comparatively, using the proposed method, the instability of the interconnected system can be identified once the leading LOSP ($\mathrm{DLP_{XYRD}}$) occurs, but the inter-area instability and $\boldsymbol{\eta}_{\mathrm{sys}}$ cannot be obtained until the last DLP ($\mathrm{DLP_{LC1}}$) occurs. This fully proves that the stability judgment of the system is independent of the identification of both the inter-area instability and calculation of $\boldsymbol{\eta}_{\mathrm{sys}}$ when using the proposed method in TSA.

D. PROPOSED METHOD (NOT-ALL-CRITICAL-MACHINES MONITORING)

From the analysis in Section C, theoretically, the inter-area instability can be identified only when the last DLP in SYSTEM_LC, i.e., $\mathrm{DLP_{LC1}}$ occurs. However, in real online security control, at the instant $\mathrm{DLP_{LCR1}}$ occurs, the system operator can comprehend that SYSTEM_LC is severely disturbed, as most critical machines (six machines) in SYSTEM_LC have already become unstable. In this grim situation, the system operator might terminate monitoring the rest of the critical machines and give up identifying inter-area instability. Further, forceful proactive controlling actions

may be enforced in SYSTEM_LC as most critical machines in SYSTEM_LC are already identified to become unstable.

E. SEPARATION OF A PAIR OF MACHINES

From the analysis in the first paper [1], an individual machine in the COI reference is an IVCS that is formed by a ''pair'' of machines in synchronous reference, i.e., the individual machine and the virtual COI machine. In the following analysis, we further demonstrate the mechanisms of the IEEAC method and that of the proposed method in synchronous reference. The trajectories of the COI machines (Machine A, Machine S and the virtual COI machine) in synchronous reference are shown in Fig. 20. Notice that the rotor angles of the machines in SYSTEM_SD are not shown in the figure.

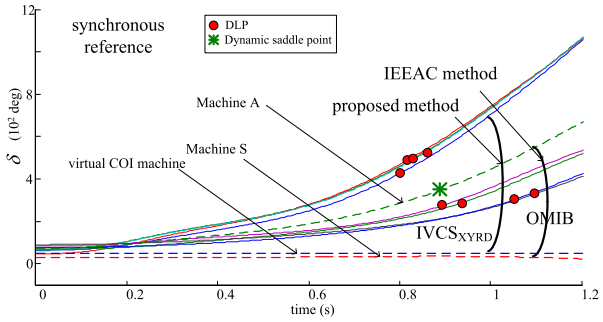

FIGURE 20. Separation between a pair of machines [TS-3, line-LIAOC_TANZ, 0.22s].

It can be seen from Fig. 20 that both the IEEAC method and the proposed method depict the power system transient stability via the separation of a *pair* of machines. The only difference between them is the formation of the pairs. To be specific, for the IEEAC method, the inter-area instability of the interconnected system is depicted as the separation between a ''pair'' of equivalent machines, i.e., Machine A and Machine S which are equivalent machines of the two regional systems. Comparatively, using the proposed method, the inter-area instability is depicted as the separation between eight ''pairs'' of machines, i.e., the pairs formed by eight individual machines in SYSTEM_LC and the virtual COI machine. Moreover, using the proposed method, the instability (not the inter-area instability) of the interconnected system can be directly depicted by the separation of only *one* pair of machines.

From Fig. 20, the rotor angles of Machine S and those of the virtual COI machine are quite close because the non-critical machines in SYSTEM_SD are the majority after fault clearing. Therefore, since Machine A is the equivalent of all machines in SYSTEM_LC, the dynamic saddle point in the OMIB system can also be seen as an ''equivalent'' of the DLPs of all the critical machines in SYSTEM_LC, as shown in Fig. 20. This can explain the reason why when using the proposed method in TSA, the instability of the interconnected system can be determined earlier, while the inter-area instability is identified later than when using the IEEAC method.

X. FURTHER ANALYSIS OF THE NOT-ALL-CRITICAL MACHINES CHARACTERISTIC OF THE PROPOSED METHOD

Compared with the global methods that observe the transient behavior of all machines in the system, the proposed method only focuses on the stability of critical machines by neglecting that of the non-critical machines. This is also the reason why the proposed method is named as an ''individual machine'' method.

The ''individual machine'' in the proposed method may still be controversial for the global analysts because it seems that the stability judgment of a critical machine is ''isolated'' from the system. To illustrate the fundamental mechanism of the proposed method more explicitly and clearly, the following statements are outlined as below.

a: THE TRANSIENT STABILITY OF THE SYSTEM IS A ''GLOBAL'' PROBLEM

In the transient stability of a multimachine system, all the machines in the system, whether they are critical machines or non-critical machines, have complicated interactions with each other. Thus, the transient stability of the system is an unquestionable global problem.

b: OBSERVING THE TRANSIENT STABILITY OF THE SYSTEM MAY BE AN ''INDIVIDUAL MACHINE'' PROBLEM

Although the transient stability of the multimachine system is a global problem and all machines interact with each other, only a few critical machines finally separate from the system and cause the system to become unstable after the fault is cleared. Therefore, the proposed method may only focus on the stability of each ''individual'' critical machine rather than all machines in the system, making the method ''nonglobal''. In fact, the term ''nonglobal'' and ''individual'' in the proposed method are only used to describe the way of observing the transient stability of the system, rather than depicting the interactions of all machines in the system.

To understand the relationship between the global and individual-machine concepts, a further explanation about the parameters in an individual machine is merited in a 3DKC. In the 3DKC of Machine i, the f_i comprises the angles of all machines in the system. This means that the whole system trajectory is already implicated in the 3DKC. A demonstration regarding the implication of the system trajectory in the 3DKC of an individual machine is shown in Fig. 21.

From the analysis above, all critical machines interact with each other in the transient stability of the multimachine system. The IMEAC method only observes the transient stability of the system in an individual-machine way.

XI. THE JIGSAW THINKING IN THE PROPOSED METHOD

The individual-machine characteristic of the proposed method can be tutorially expressed by a boy playing with a jigsaw puzzle, as shown in Fig. 22.

In Fig. 22, when the boy picks up Piece 2 first, he does not know what the other pieces look like. However, he knows the

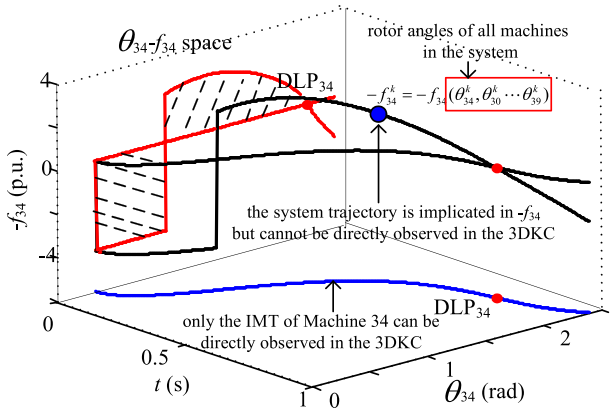

FIGURE 21. The implication of the system trajectory in the 3DKC of an individual machine [TS-1, bus-34, 0.202s].

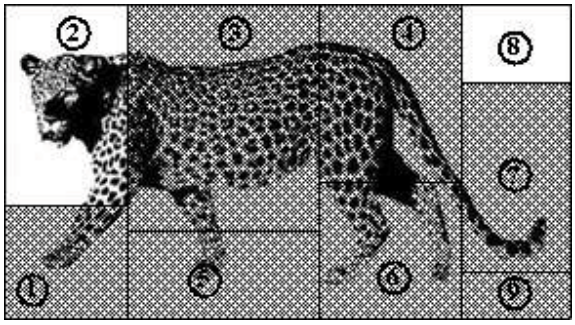

FIGURE 22. A leopard jigsaw puzzle illustrating the mechanism of the proposed method.

piece in hand is the head of the leopard; thus, he ascertains that the underlying object in the figure is a leopard. When he picks up Piece 8 first, he knows that the blank piece is a part of the jigsaw. Unfortunately, he is unable to figure out what he is playing as the piece in hand is blank. Therefore, if the boy only wants to determine the figure he is forming, any piece among Pieces 1-7 could provide a clear indication that the figure is a leopard. However, if the boy wants to know what the whole jigsaw really looks like, he needs to collect all the pieces, including Pieces 8 and 9.

We map the jigsaw puzzle into the transient stability analysis of the proposed method. Pieces 1-7 represent the unstable critical machines, and Pieces 8-9 represent the stable critical machines. The whole jigsaw puzzle represents the set of all critical machines (including the stable ones) in the system.

After fault clearing, once the operator first judges that Machine 2 has become unstable without observing the stability of other critical machines, then the system is judged as becoming unstable. Once the operator first judges that Machine 8 is stable, neglecting other critical machines, then the method does not know whether the system is stable or not because the stability of the other critical machines is still unknown. However, since Machine 8 is also a critical machine, it is also ''one piece of the jigsaw puzzle'', although it is blank. Therefore, if the operator only wants to know whether the system is stable or not, finding any one unstable machine among Machines 1 to 7 would confirm the instability of the system. If the operator wants to know the MOD or the stability margin of the whole system, he needs to observe all the critical machines in the system, including Machines 8 and 9.

XII. DISCUSSION AND CONCLUSIONS

This paper applies the proposed direct-time-domain method for TSA and CCT computation. The stability margin of the system is defined as a vector with its components being the stability margins of all the critical machines. This definition can facilitate parallel monitoring of the critical machines in TSA. In addition, this definition further leads to the concept of the nonglobal stability margin, which allows the system operators to give up monitoring some critical machines if they have already comprehended the key transient characteristics of the system. Especially, for the CCT computation, only the MDM is monitored, wherein the nonglobal monitoring for the MDM is effective for grasping the transition of the system from being stable to being unstable. It is also clarified that the MDM and LUM might be two different machines for some cases.

Compared with the CUEP method, the proposed method can directly identify the MOD via the stability identification of each critical machine of the system. Compared with the IEEAC method, the proposed method also depicts the transient instability of the system through the separation of pairs of machines. However, the essential difference between the two methods is the formation of the pairs.

REFERENCES

[1] S. Wang, J. Yu, and W. Zhang, "Transient stability assessment using individual machine equal area criterion Part I: Unity principle," *IEEE Access*, to be published, doi: 10.1109/ACCESS.2018.2854227.
[2] S. E. Stanton and W. P. Dykas, "Analysis of a local transient control action by partial energy functions," *IEEE Trans. Power Syst.*, vol. 4, no. 3, pp. 996–1002, Aug. 1989.
[3] S. E. Stanton, "Transient stability monitoring for electric power systems using a partial energy function," *IEEE Trans. Power Syst.*, vol. 4, no. 4, pp. 1389–1396, Nov. 1989.
[4] P. Rastgoufard, A. Yazdankhah, and R. A. Schlueter, "Multi-machine equal area based power system transient stability measure," *IEEE Trans. Power Syst.*, vol. PWRS-3, no. 1, pp. 188–196, Feb. 1988.
[5] M. H. Haque, "Further developments of the equal-area criterion for multimachine power systems," *Electr. Power Syst. Res.*, vol. 33, pp. 175–183, Jun. 1995.
[6] A. A. Fouad, V. Vittal, and T. K. Oh, "Critical energy for direct transient stability assessment of a multimachine power system," *IEEE Trans. Power App. Syst.*, vol. PAS-103, no. 8, pp. 2199–2206, Aug. 1984.

SONGYAN WANG received the B.S., M.S., and Ph.D. degrees from the School of Electrical Engineering and Automation, Harbin Institute of Technology (HIT), in 2007, 2009, and 2012, respectively. He was a Visiting Scholar with Virginia Tech, Blacksburg, VA, USA, in 2010. From 2013 to 2014, he was a Research Fellow with the Queen's University Belfast, U.K. He is currently an Assistant Professor with HIT. His research interests include power system operation and control.

Dr Wang is an Associate Editor of the Renewable and Sustainable Energy Reviews.

JILAI YU joined the School of Electrical Engineering and Automation, Harbin Institute of Technology, in 1992. From 1994 to 1998, he was an Associate Professor with the School of Electrical Engineering and Automation, Harbin Institute of Technology, where he is currently a Professor and the Director of Electric Power Research Institute. His current research interests include power system analysis and control, optimal dispatch of power system, green power, and smart grid.

WEI ZHANG (S'11–M'14) received the B.S. and M.S. degrees in power system engineering from the Harbin Institute of Technology, Harbin, China, in 2007 and 2009, respectively, and the Ph.D. degree in electrical engineering from New Mexico State University, Las Cruces, NM, USA, in 2013.

He is currently an Associate Professor with the School of Electrical Engineering and Automation, Harbin Institute of Technology, Harbin, Heilongjiang, China. His research interests include distributed control and optimization of power systems, renewable energy and power system state estimation, and stability analysis.